

Dynamic Count Models with Flexible Innovation Processes for Irregular Maritime Migration

Gregor Zens* Jakub Bijak[†]

August 2025

Abstract

Motivated by the dynamics of weekly sea border crossings in the Mediterranean (2015–2025) and the English Channel (2018–2025), we develop a Bayesian dynamic framework for modeling potentially heteroskedastic count time series. Building on theoretical considerations and empirical stylized facts, our approach specifies a latent log-intensity that follows a random walk driven by either heavy-tailed or stochastic volatility innovations, incorporating an explicit mechanism to separate structural from sampling zeros. Posterior inference is carried out via a straightforward Markov chain Monte Carlo algorithm. We compare alternative innovation specifications through a comprehensive out-of-sample density forecasting exercise, evaluating each model using log predictive scores and empirical coverage up to the 99th percentile of the predictive distribution. The results of two case studies reveal strong evidence for stochastic volatility in sea migration innovations, with stochastic volatility models producing particularly well-calibrated forecasts even at extreme quantiles. The model can be used to develop risk indicators and has direct policy implications for improving governance and preparedness for sea migration surges. The presented methodology readily extends to other zero-inflated non-stationary count time series applications, including epidemiological surveillance and public safety incident monitoring.

Keywords: zero-inflated Poisson; Bayesian dynamic models; migration time series; density forecasting; heavy-tailed innovations

*Population and Just Societies Program, International Institute for Applied Systems Analysis (IIASA), Laxenburg, Austria. Corresponding author: zens@iiasa.ac.at.

[†]Department of Social Statistics and Demography, University of Southampton, Southampton, United Kingdom. J.Bijak@soton.ac.uk.

1 Introduction

Irregular maritime migration and border crossings are major issues in contemporary political discourse and come with severe humanitarian consequences due to the high mortality risks associated with sea migration routes. At the same time, such "small boat" passages constitute one of the few migration flows that can be tracked with relative precision, based on systematic search-and-rescue logs, coastguard interceptions, and immigration or asylum registration systems in arrival countries. The resulting availability of high-frequency data should, in principle, enable a rigorous statistical investigation.

However, the literature on modeling the dynamics of irregular maritime migration and border crossings remains surprisingly thin. This gap may stem from two intertwined obstacles. First, data on irregular arrivals by sea present unique challenges, as high-frequency counts of migrant arrivals are noisy, non-stationary, volatile, and often zero-inflated – a combination that overwhelms many off-the-shelf modeling techniques. Second, these characteristics make point forecasts notoriously unreliable, potentially creating the impression that any attempt to effectively model irregular maritime border crossings is futile. This leaves a significant research gap both in terms of forecasting capabilities that could enhance preparedness and humanitarian response, and in terms of developing structural insights into the underlying drivers and dynamics of irregular maritime migration.

In this article, we demonstrate that both meaningful structural insights and well-calibrated density forecasts of sea border crossing activity can be obtained using a context-specific probabilistic model. Based on theoretical considerations and stylized empirical facts of irregular maritime border crossing data, we develop a Bayesian dynamic modeling framework for count data time series. This framework is designed for discrete time series jointly characterized by (i) non-stationarity in the mean, (ii) volatility clustering or sudden shifts in the log-scale intensity, and (iii) zero-inflation. We develop a simple Markov chain Monte Carlo (MCMC) algorithm for posterior simulation. The proposed methods and algorithms are flexible, easily extendable, and applicable to any non-negative integer time series, suggesting their broader utility across various fields beyond modeling irregular sea border crossings.

We apply the model to two case study datasets on weekly maritime border crossings in the Mediterranean Sea and in the English Channel. We benchmark various versions of the model to gain insight into irregular migration dynamics, focusing particularly on the problem of producing and evaluating density forecasts. Specific emphasis is placed on empirical coverage in the tails of the predictive density of maritime border crossings. This focus is especially important, as accurate tail probability forecasts directly enhance preparedness for extreme events. Well-calibrated predictive distribution tails also enable more effective contingency planning in the context of irregular migration, which is often characterized by rare events of high magnitude (see e.g. [Bijak, 2024](#)).

Our results indicate that the dynamics of irregular sea border crossings are effectively captured by a Poisson state-space model with a random-walk log intensity with persistent time-varying innovation volatility. In both our case studies, this

model most accurately characterizes irregular sea border crossing activity and generates well-calibrated one-week-ahead predictive densities with precise empirical coverage extending to extreme tail quantiles such as q_{95} and q_{99} . We connect these findings with the underlying theoretical considerations and discuss implications for policy and future empirical research under the assumption that sea border crossings do indeed follow a random walk with persistent time-varying volatility.

This article therefore offers two primary contributions. First, we introduce a flexible model for analyzing potentially zero-inflated non-stationary count data time series using a dynamic latent variable framework, accompanied by a straightforward computational algorithm for sampling from the posterior distribution. This advances the literature on Bayesian approaches to dynamic modeling of complex integer-valued time series. Second, we conduct the first comprehensive predictive evaluation to determine effective approaches for probabilistic modeling of irregular maritime border crossing data through two high-profile and policy-relevant case studies. This yields a new benchmark model for examining such processes and generates evidence-based policy insights regarding the underlying structural dynamics.

The remainder of the article is structured as follows. Section 2 presents the motivating case study data sets, empirical stylized facts, theoretical considerations, and related literature. Section 3 presents our model, prior specification, and the computational approach. Section 4 applies the methodology to the case study data sets. Section 5 discusses the policy implications of the results and concludes with directions for future research.

2 Data, Stylized Facts, and Theoretical Considerations

We analyze weekly time series data on irregular sea border crossings across two distinct geographical regions. The first case study examines irregular arrivals in Italy across the Mediterranean Sea, encompassing $T = 494$ weeks from 2015W40 to 2025W11. These data are sourced from the *Operational Data Portal* of the United Nations High Commissioner for Refugees (UNHCR)¹. On average, we observe 1,607 arrivals per week, with a weekly median of 851 arrivals. The series ranges from zero arrivals up to a maximum of 15,694 arrivals in the week of August 29, 2016.

For our second case study, we investigate irregular arrivals by sea to the United Kingdom across the English Channel, covering $T = 376$ weeks from 2018W01 to 2025W11. This dataset is provided by the Border Force branch of the UK Home Office². On average, we observe 413 arrivals per week, with a weekly median of 152 arrivals. The series ranges from zero arrivals up to a maximum of 3,564 arrivals in the week of August 22, 2022.

¹Source: <https://data.unhcr.org/en/situations/europe-sea-arrivals/location/24521> (as of 7 August 2025).

²Source: <https://www.gov.uk/government/publications/migrants-detected-crossing-the-english-channel-in-small-boats/migrants-detected-crossing-the-english-channel-in-small-boats-last-7-days> (as of 7 August 2025).

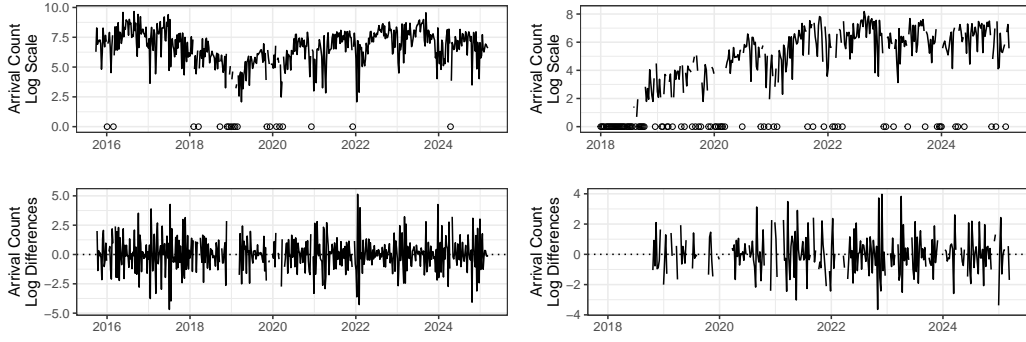


Figure 1: Irregular maritime border crossing case study data sets. Left: Mediterranean Sea border crossings to Italy by sample week from 2015W40 to 2025W11. Right: English Channel crossings by sample week from 2018W01 to 2025W11. Top panels display log-transformed counts, with zero counts highlighted separately as dots on the zero line. Bottom panels show log differences of counts for observations where both $y_t > 0$ and $y_{t-1} > 0$.

2.1 Empirical Stylized Facts and Theoretical Considerations

Figure 1 presents the data after a logarithmic transformation (top panels) and after taking first differences of the log transformed counts (bottom panels). The untransformed count time series are shown in Figure S1 in the supplementary material. From a modeling perspective, Figure 1 highlights the three main challenges inherent in capturing boat migration time series dynamics.

First, as is common in many migration processes (Bijak, 2010), the count-valued data exhibit non-stationarity with respect to mean intensity. While crossing conditions typically lead to somewhat higher activity in summer months than winter, there is no clear deterministic trend over the full time period. To address this non-stationarity, we will specify a benchmark count time series model that allows for random walk behavior of the log intensity parameter. The random walk assumption is empirically further supported given the log differences in the bottom panels in Figure 1 are almost exclusively centered around the zero line, suggesting the absence of a deterministic drift.

Second, as becomes evident from the time series of log differences, the innovation process on the log scale is likely heteroskedastic. A priori, it is unclear whether this heteroskedasticity is the result of an overall heavy-tailed (but constant in time) process, or whether the volatilities themselves are following a dynamic process that produces persistently time-varying volatilities that may be clustered in time. To investigate this, we will specify and compare various volatility models empirically and benchmark them against each other in a large-scale pseudo-out-of-sample forecasting exercise.

Third, observed zero counts may reflect one out of two distinct phenomena. On the one hand, zero arrivals may be the result of weeks where external circumstances – such as coast guard operations, adverse weather conditions, or low smuggler availability – temporarily prevent crossings despite relatively high migration intensity in

surrounding weeks (compare the zero counts after 2022 in the UK time series). In other cases, zero counts may stem from genuinely low migration intensity during those periods (such as in the early period of the UK data). There is no clear way to *a priori* classify a zero as an unexpected ‘outlier’ which can be treated as missing when modeling migration intensity versus treating a zero as an important data point that informs the model about low migration activity in certain time periods. This motivates an approach that treats the probability of crossing and the intensity of the underlying migration process as two separate, but interacting processes that jointly generate the observed arrival counts. This conceptualization naturally leads to a parameter-driven time series model for zero-inflated counts.

Importantly, the empirical patterns in Figure 1 – non-stationarity, heteroskedasticity and zero-inflation – are consistent with what one would expect from irregular migration processes that result from a complex interplay of individual decisions, weather conditions, smuggling operations, border enforcement (including push-backs and deportations), political and diplomatic solutions, and many more factors (see e.g. [Rodríguez Sánchez et al., 2023](#); [Frontex, 2024](#); [Migration Observatory, 2025](#)). These migration drivers can be conceptualized as evolving approximately as first-order random walks whose innovation variances can evolve over time – dynamics that are reasonable to assume for classical migration drivers (such as conflict pressures, environmental disasters, macroeconomic shocks, smuggler capacity, or border enforcement), the effects of which may be difficult to quantify. In such instances, random walk models, possibly with stochastic volatility, have been proposed as atheoretical alternative options for analyzing migration in the absence of precise knowledge on drivers ([Bijak, 2010](#)). If these latent drivers combine to determine migration intensity through some form of interaction, this may naturally produce the observed non-stationary local trending and heteroskedasticity in the migration intensity itself. Occasional extreme events may temporarily suppress migration activity entirely, giving rise to potential zero-inflation. Although these considerations align our three stylized facts – and ultimately, our statistical model – with basic theoretical intuition, a completely formalized and consistent micro-theoretical treatment of irregular sea migration is largely absent from the literature. Developing such a framework is left for future research.

2.2 Existing Statistical Approaches

Conceptual statistical work on high-frequency irregular sea migration data remains relatively scarce. The majority of quantitative literature in this domain focuses on causal inference studies that evaluate the impact of search-and-rescue operations, coast guard activity, environmental conditions, or riots in harbor cities on migration patterns or smuggler network behavior ([Camarena et al., 2020](#); [Hoffmann Pham and Komiyama, 2024](#); [Friebel et al., 2024](#); [Deiana et al., 2024](#)). These studies typically employ relatively simplistic regression structures for count data or Gaussian models for log-transformed counts, with regression specifications following either basic structures with few covariates or gravity-type models. Predictive evaluations are infrequent and, if provided, focus exclusively on point prediction accuracy.

In parallel with recent efforts to apply machine learning techniques for predicting irregular migration activity (Carammia et al., 2022), several studies have attempted to forecast boat migration across various frequencies and case studies – often focusing on Mediterranean border crossings – using an array of machine learning and standard time series analytical tools, sometimes combined in ensembles (Georgiou, 2016; Bosco et al., 2024). While these studies demonstrate some level of point predictability in monthly border crossing data, the fitted models are largely black-box approaches that provide limited evidence-based structural insights into underlying patterns and typically do not evaluate density forecasts. Bridging the gap between purely causal inference-oriented and purely prediction-oriented work, Rodríguez Sánchez et al. (2023) used Bayesian hierarchical time series models to compare various predictions for Mediterranean small boat migration activity. The authors generated counterfactual predictions to address causal inference questions related to the role of search and rescue operations, which were found not to influence irregular migration flows. Their work also employed spike-and-slab priors for variable selection in regression models, demonstrating the broader utility of Bayesian methods for migration modeling.

In substantive terms, we identify three key limitations in existing statistical approaches to irregular maritime migration. First, irregular migration is typically modeled using similar frameworks as regular migration flows (e.g., labor mobility), despite fundamentally different underlying dynamics. In addition, even for regular migration dynamics, these conventional models often demonstrate poor predictive performance (Beyer et al., 2022). Second, many existing forecasts, including those using machine learning methods, rely almost exclusively on point forecast metrics, neglecting probabilistic accuracy measures related to the calibration of the distributions. The latter are essential for uncertainty quantification and risk assessment. Third, maritime migration patterns are almost exclusively analyzed in the context of the Mediterranean Sea, limiting our understanding of whether observed dynamics are region-specific or reflect more universal patterns in irregular maritime migration. In general, little is known about the dynamics and structure of irregular maritime migration data from a statistical perspective.

Our work addresses these gaps and hence makes several contributions to the literature. First, we construct a parsimonious probabilistic model tailored specifically to high-frequency irregular migration counts, grounded in both theoretical reasoning and observed empirical patterns. Despite requiring no covariates, this framework generates accurate density forecasts and yields insights relevant to policy design. Second, we pioneer the evaluation of density forecast accuracy in this domain, with special emphasis on tail behavior—critical for evaluating uncertainty and risk assessments. Third, we provide the first analysis of the English Channel crossings alongside Mediterranean routes, broadening the empirical evidence base. More broadly speaking, the dynamic modeling framework we develop extends naturally to applications beyond migration, including epidemiological analyses, accident modeling or reliability contexts.

3 Dynamic Zero-Inflated Heteroskedastic Count Models

3.1 Model specification

Let $y_t \in \mathbb{N}_0$ denote a univariate count observed at equally-spaced times $t = 1, \dots, T$. Each count can be a *structural* zero or arise from a *sampling* mechanism. Introduce the latent indicator $s_t \in \{0, 1\}$ with interpretation $s_t = 0$ (structural zero) and $s_t = 1$ (sampling path active). Conditionally on s_t and a latent log-intensity $z_t \in \mathbb{R}$ the data-generating process is

$$y_t \mid s_t, z_t \sim \begin{cases} \delta_0, & s_t = 0, \\ \mathcal{P}(\lambda_t), & s_t = 1, \end{cases} \quad \lambda_t = \exp(z_t), \quad t = 1, \dots, T, \quad (3.1)$$

where δ_0 denotes a point mass at zero. The binary indicators are taken to be i.i.d. $s_t \sim \text{Bernoulli}(\pi)$, $\pi \in (0, 1)$. More elaborate dynamic choices are possible but are not pursued here. Marginalizing over the indicator yields the zero-inflated Poisson mixture

$$p(y_t \mid z_t) = \begin{cases} (1 - \pi) + \pi \exp(-\lambda_t), & y_t = 0, \\ \pi \frac{\lambda_t^{y_t}}{y_t!} \exp(-\lambda_t), & y_t \geq 1, \end{cases} \quad \lambda_t = \exp(z_t). \quad (3.2)$$

The latent³ state evolves as a random walk

$$z_t = z_{t-1} + \varepsilon_t, \quad \varepsilon_t \stackrel{\text{i.i.d.}}{\sim} f_\varepsilon(\cdot; \vartheta), \quad t = 1, \dots, T, \quad (3.3)$$

with density f_ε parametrized using hyper-parameters ϑ .

For f_ε , four distinct specifications are considered. As a simple benchmark, we use the homoskedastic Gaussian case $f_\varepsilon = \mathcal{N}(0, \sigma^2)$. For constant heavy-tailed densities, we consider a scaled t-density with ν degrees of freedom $f_\varepsilon = t_\nu(0, \sigma^2)$ and a scale mixture of two Gaussian densities $f_\varepsilon = \sum_{h=1}^2 \eta_h \mathcal{N}(0, \sigma_h^2 \sigma^2)$ with $\eta_1 + \eta_2 = 1$. Finally, following [Bijak \(2010\)](#), to model persistent time-varying volatility patterns, we consider a stochastic volatility model ([Kastner, 2016](#)) $f_\varepsilon = \mathcal{N}(0, \exp(h_t))$ where $h_t = \mu + \phi(h_{t-1} - \mu) + \xi_t$ and $\xi_t \sim \mathcal{N}(0, \sigma_\xi^2)$.

The considered model is essentially a heteroskedastic non-Gaussian state-space model. Poisson state-space formulations and their extensions are well-known in the Bayesian literature ([West et al., 1985](#); [Frühwirth-Schnatter and Wagner, 2006](#); [Berry and West, 2020](#)), and state-space models have been used in migration-related applications in a handful of studies (e.g. [Rodríguez Sánchez et al., 2023](#); [Zens and Thalheimer, 2025](#)). Poisson state-space models with a random-walk log

³Note that the underlying factors driving sea migration are extremely challenging to model explicitly. Consider for instance only conflict as a single potential driver of irregular migration. Data on conflict is available in a timely, geocoded format, which is already a major benefit compared to measurements of other potential drivers, enabling detailed modeling of conflict-related displacement (see e.g. [Zens and Thalheimer, 2025](#)). At the same time, accounting for the activity of the smuggling gangs, time lag due to travel to the point of embarkation and the waiting time there is essentially a black box. Hence, a latent variable model is highly useful in this context.

intensity augmented with locally adaptive shrinkage or dynamic horseshoe priors have been applied to trend filtering in count series (Kowal et al., 2019; Schafer and Matteson, 2025), differenced zero-inflated negative binomial specifications have been used to capture time-varying dispersion in high-frequency financial counts (Barra et al., 2018), and spatially varying-dispersion frameworks have been considered in epidemiological settings (e.g. Mutiso et al., 2022). In general, coupling count-data likelihoods with state-space methods enables the construction of highly intricate, domain-specific models (e.g. Kim and Albert, 2018). Our proposed framework builds directly on these developments, offering a simple, flexible, and easily extendable approach to zero-inflated, heteroskedastic count time series with flexible innovation densities, where inference can be carried out via a straightforward MCMC algorithm. For comprehensive overviews of count time-series methodology, see Jung et al. (2006) or Davis et al. (2016). For a Bayesian treatment of static zero-inflated count models with overdispersion, see Neelon (2019).

3.2 Prior Specification

Bayesian inference requires elicitation of suitable prior densities. In this article, we aim for at most weakly informative prior specifications to avoid that our conclusions rely heavily on specific hyperparameter choices. We use a Jeffreys prior $\pi \sim \mathcal{B}(0.5, 0.5)$ for the probability of observing a sampling count. The prior on the initial value of the latent log intensity is chosen to be flat $p(z_0) \propto 1$. For scaling parameters, proper and conditionally conjugate inverse Gamma priors $\sigma^2, \sigma_h^2 \sim \mathcal{IG}(2.5, 1.5)$ are specified. In the Student-t model, we will estimate the degrees of freedom parameter from the data jointly alongside the other parameters. For this, we pick a shifted exponential prior with rate 1/6 and shifted to values larger than 3 for ν to ensure at least the first three moments of the innovation density exist. For the mixture model weights, we assume $(\eta_1, \eta_2) \sim \text{Dirichlet}(1, 1)$, allowing for conditionally conjugate posterior updates. Finally, for the stochastic volatility model, we follow the default choices in Kastner (2016) and specify $\mu \sim \mathcal{N}(0, 100)$, $(\phi + 1)/2 \sim \mathcal{B}(5, 1.5)$ as well as $\sigma_\xi^2 \sim \mathcal{G}(0.5, 0.5)$.

3.3 Posterior Simulation

Let

$$\mathbf{z} = (z_1, \dots, z_T)^\top, \quad \mathbf{s} = (s_1, \dots, s_T)^\top$$

collect the latent states and inclusion indicators corresponding to the data y_1, \dots, y_T . We use $\boldsymbol{\vartheta}$ to denote all hyper-parameters associated with a particular choice of f_ε . To sample from the joint posterior

$$p(\mathbf{z}, \mathbf{s}, \boldsymbol{\vartheta}, z_0, z_{T+1}, \pi \mid \mathbf{y}),$$

we construct a simple Gibbs–Metropolis sampler that cycles through each full conditional in turn. After choosing starting values and discarding an initial burn-in, repeated iteration yields valid draws from the target posterior. Note that we

explicitly include both the initial value z_0 and the one-step-ahead forecast z_{T+1} as unknown parameters to simplify the exposition below.

i. Updating (z_0, z, z_{T+1}) . Consider the random-walk prior $z_t = z_{t-1} + \varepsilon_t$ with an innovation density f_ε that admits a conditional-Gaussian representation. The augmented state vector (z_0, z, z_{T+1}) is then a priori jointly Gaussian (Chan and Jeliazkov, 2009) with zero mean and (singular) precision matrix

$$P(\vartheta) = D^\top K(\vartheta) D, \quad D = \begin{pmatrix} -1 & 1 & & & \\ & -1 & 1 & & \\ & & \ddots & \ddots & \\ & & & -1 & 1 \end{pmatrix}_{(T+1) \times (T+2)},$$

where $K(\vartheta) = \text{diag}(k_1, \dots, k_{T+1})$ collects the precision parameters of the increments. The exact form of $K(\vartheta)$ depends on the chosen specification for f_ε and will be detailed later. The posterior kernel factorizes into this (improper) Gaussian prior and the Poisson likelihood contributions of those observations that are included in the sampling path ($s_t = 1$):

$$p(z_0, z, z_{T+1} \mid \mathbf{y}, \mathbf{s}, \vartheta) \propto \mathcal{N}_{T+2}(\mathbf{0}, P(\vartheta)^{-1}) \prod_{t: s_t=1} \mathcal{P}(y_t; \exp(z_t)).$$

Drawing directly from this joint density is difficult, so we proceed by single-site updates $p(z_t \mid \mathbf{z}_{-t}, s_t, y_t, \vartheta)$ for $t = 0, \dots, T+1$, where \mathbf{z}_{-t} collects all latent log-intensities except z_t . Because the prior is multivariate Gaussian, these conditionals are

$$p(z_t \mid \mathbf{z}_{-t}, s_t, y_t, \vartheta) \propto \begin{cases} \mathcal{N}(z_t; m_t, v_t), & s_t = 0, \\ \mathcal{N}(z_t; m_t, v_t) \mathcal{P}(y_t; \lambda_t), & s_t = 1, \end{cases} \quad \lambda_t = e^{z_t}.$$

where we treat z_0 and z_{T+1} as missing and hence implicitly fix $s_0 = 0$ and $s_{T+1} = 0$. The conditional moments m_t and v_t immediately follow from the properties of the multivariate Gaussian distribution

$$m_t = -\frac{1}{P_{tt}} \sum_{j \neq t} P_{tj} z_j, \quad v_t = \frac{1}{P_{tt}}$$

where P_{tj} denotes element $[t, j]$ in $P(\vartheta)$. Each of the univariate conditionals is a proper density, and we sample z_t using an adaptive Metropolis-Hastings step (Roberts and Rosenthal, 2009) that gradually diminishes adaptation of the proposal variance during MCMC and targets an acceptance rate of 0.234. The Poisson term $\mathcal{P}(y_t; \lambda_t)$ dominates whenever y_t is relatively large, effectively collapsing the conditional to a near point mass. In the empirical examples considered below we thus did not encounter MCMC efficiency problems due to employing single-site updates.

ii. Updating s . To update the indicators s_t , fix $s_t = 1$ for all t where $y_t > 0$. For observations where $y_t = 0$, sample s_t from the conditional posterior $p(s_t | y_t, z_t, \pi)$. Recall that the prior probability of the sampling path being active is π and that $p(y_t = 0 | z_t) = \mathcal{P}(0; \lambda_t) = \exp(-\lambda_t)$. Using Bayes' theorem, the conditional posterior $p(s_t | y_t, z_t, \pi)$ is hence Bernoulli with

$$p(s_t = 1 | y_t, z_t, \pi) = \frac{\pi \exp(-\lambda_t)}{(1 - \pi) + \pi \exp(-\lambda_t)} \quad \lambda_t = \exp(z_t).$$

iii. Updating π . The conditional posterior density $p(\pi | s)$ is a Beta density $\pi \sim \mathcal{B}(0.5 + \sum_{t=1}^T s_t, 0.5 + T - \sum_{t=1}^T s_t)$.

iv. Updating ϑ . The hyperparameter updates depend on the choice of the innovation density f_ε . We present the posterior updates for four distributional assumptions below.

Option 1: Gaussian Innovations When $\varepsilon_t \sim \mathcal{N}(0, \sigma^2)$, the variance has a conjugate inverse-gamma posterior:

$$\sigma^2 | z \sim \mathcal{IG}\left(2.5 + \frac{T+1}{2}, 1.5 + \frac{1}{2} \sum_{t=1}^{T+1} (z_t - z_{t-1})^2\right),$$

For the latent precision updates, set $k_t = \sigma^{-2}$ for all t .

Option 2: Student- t Innovations Let $\Delta z_t = z_t - z_{t-1}$. We employ the scale mixture representation of the Student- t distribution:

$$\Delta z_t | \omega_t, \sigma^2 \sim \mathcal{N}\left(0, \frac{\sigma^2}{\omega_t}\right), \quad \omega_t | \nu \sim \mathcal{G}\left(\frac{\nu}{2}, \frac{\nu}{2}\right),$$

with prior $\nu - 3 \sim \text{Exp}(1/6)$ ensuring the first three moments of the prior density exist. The resulting conditional posteriors are:

$$\begin{aligned} \sigma^2 | \omega, z &\sim \mathcal{IG}\left(2.5 + \frac{T+1}{2}, 1.5 + \frac{1}{2} \sum_{t=1}^{T+1} \omega_t \Delta z_t^2\right), \\ \omega_t | \nu, \sigma^2, z &\stackrel{\text{i.i.d.}}{\sim} \mathcal{G}\left(\frac{1+\nu}{2}, \frac{\nu}{2} + \frac{\Delta z_t^2}{2\sigma^2}\right), \quad t = 1, \dots, T+1. \end{aligned}$$

The degrees of freedom ν are updated via adaptive Metropolis-Hastings on the log scale. Propose $\log \nu^* \sim \mathcal{N}(\log \nu, \tau_\nu)$ and accept with probability:

$$\alpha = \min\left\{1, \frac{\nu^* p(\omega | \nu^*) p(\nu^*)}{\nu p(\omega | \nu) p(\nu)}\right\},$$

where the adaptation targets an acceptance rate of 0.234. For the latent precision updates, set $k_t = \omega_t / \sigma^2$.

Option 3: Finite Gaussian Scale Mixture Consider H mixture components with weights $\boldsymbol{\eta} = (\eta_1, \dots, \eta_H)$, component variances σ_h^2 , and allocation indicators $\rho_t \in \{1, \dots, H\}$:

$$\begin{aligned} \Delta z_t \mid \rho_t = h, \sigma^2, \sigma_h^2 &\sim \mathcal{N}(0, \sigma^2 \sigma_h^2), & \sigma_h^2 &\stackrel{\text{i.i.d.}}{\sim} \mathcal{IG}(2.5, 1.5), \\ \rho_t \mid \boldsymbol{\eta} &\sim \text{Categorical}(\boldsymbol{\eta}), & \boldsymbol{\eta} &\sim \text{Dirichlet}(1, \dots, 1). \end{aligned}$$

Define $R_h = \sum_{t=1}^{T+1} \mathbb{1}(\rho_t = h)$ as the number of allocations to component h . The resulting conditional posteriors are:

$$\begin{aligned} \sigma^2 \mid \sigma_{\rho_t}^2, \mathbf{z} &\sim \mathcal{IG}\left(2.5 + \frac{T+1}{2}, 1.5 + \frac{1}{2} \sum_{t=1}^{T+1} \sigma_{\rho_t}^{-2} \Delta z_t^2\right), \\ \Pr(\rho_t = h \mid \cdot) &\propto \eta_h \cdot \varphi(\Delta z_t; 0, \sigma^2 \sigma_h^2), \\ \boldsymbol{\eta} \mid \boldsymbol{\rho} &\sim \text{Dirichlet}(1 + R_1, \dots, 1 + R_H), \\ \sigma_h^2 \mid \cdot &\sim \mathcal{IG}\left(2.5 + \frac{R_h}{2}, 1.5 + \frac{1}{2\sigma^2} \sum_{t:\rho_t=h} \Delta z_t^2\right), \end{aligned}$$

where $\varphi(\cdot; \mu, \sigma^2)$ denotes the Gaussian probability density function with mean μ and variance σ^2 . For latent precision updates, set $k_t = (\sigma^2 \sigma_{\rho_t}^2)^{-1}$. We use $H = 2$ in the applications below.

Option 4. Stochastic volatility For the SV case we employ the auxiliary-mixture sampler of [Kim et al. \(1998\)](#), combined with the multivariate Gaussian joint density representation for state-space formulations ([McCausland et al., 2011](#)); see [Kastner \(2016\)](#) and the `stochvol` R package for an efficient software implementation. The estimated volatility pathways $\sigma_t^2 = \exp(h_t)$ can then be used to update the latent precisions by setting $k_t = \sigma_t^{-2}$.

3.4 Forecasting and Log Predictive Score Evaluation

To sample from the posterior predictive distribution of y_{T+1} , first sample $s_{T+1} \sim \text{Bernoulli}(\pi)$. If $s_{T+1} = 0$, set $y_{T+1} = 0$. Otherwise, draw z_{T+1} as described above, then sample $y_{T+1} \mid z_{T+1} \sim \mathcal{P}(\lambda_{T+1})$ with $\lambda_{T+1} = \exp(z_{T+1})$. Alternatively, to obtain the predictive distribution conditional on $s_{T+1} = 1$, simply sample z_{T+1} as above, then sample $y_{T+1} \sim \mathcal{P}(\lambda_{T+1})$ with $\lambda_{T+1} = \exp(z_{T+1})$.

To evaluate forecasts via log predictive density evaluations, one can either evaluate the full mixture representation in (3.2) at the hold-out value y_{T+1} , or evaluate the log predictive density of the Poisson component $\mathcal{P}(y_{T+1}; \exp(z_{T+1}))$ if focusing on forecasts conditional on $s_{T+1} = 1$. Given M posterior draws, the

estimated log predictive density at y_{T+1} is then given by

$$\widehat{\log p}(y_{T+1} | \mathbf{y}) = \log \left\{ \frac{1}{M} \sum_{m=1}^M p(y_{T+1} | z_{T+1}^{(m)}, s_{T+1}^{(m)}) \right\}.$$

4 Modeling Irregular Migration in the Mediterranean Sea and the English Channel

4.1 Predictive Performance and Benchmarking

Before discussing inferential results under any of the proposed models, we assess density forecasting performance under the various choices of f_ε . The goal of this exercise is not to show that any of the specifications outperforms all potential competitors in all cases, but to explore which model components (heavy tails, stochastic volatility) are necessary to provide reasonable density forecasting performance in the context of sea migration.

We conduct a benchmarking exercise where we repeatedly split the data into a training sample of length $T - 250$ and a single hold-out sample, the density of which we attempt to predict. We repeat this process 250 times, iterating through the time series in a rolling window format. For each model, we collect 50,000 posterior samples after an initial burn-in period of 5,000 iterations. We subsequently evaluate various performance metrics including log-predictive density evaluations, root mean square error, and correlations of posterior mean forecasts versus true values on the log scale. For tail forecast evaluation, we also assess predictive empirical coverage at the tail quantiles q_{01} , q_{05} , q_{10} , q_{90} , q_{95} , and q_{99} at the log scale.

The main results are summarized in Table 1. As we are interested in operationalizing the results conditional on observing any migration and accurate modeling of the upper tail of the density, these results are based on predictive densities conditional on $s_{T+1} = 1$ (i.e., assuming the next period is not a structural zero) and evaluation of out-of-sample metrics based on data points where $y_t > 0$. For completeness, prediction results including uncertainty surrounding s_{T+1} and including all hold-out data points are provided in Table S1. These results lead to similar conclusions, but show slightly worse empirical tail coverage probabilities, especially in the lower tail.

The results confirm our initial assessment that accurate point predictions for irregular sea border crossings are difficult to produce. The generally low correlation of point forecasts with true values highlights the poor point predictability of the irregular border crossing process, reinforcing our decision to emphasize density predictions.

For the Italian data, our results show that specifications with heavy-tailed distributions – whether through mixture models or t -distributions – outperform the basic homoskedastic Gaussian benchmark in terms of log predictive density evaluations and coverage metrics. However, the strongest performance in both case studies is obtained from specifications incorporating stochastic volatility, which

Table 1: Results of the Predictive Exercise and Hold-out Evaluation.

		LPS	RMSE	Corr.	q_{01}	q_{05}	q_{10}	q_{90}	q_{95}	q_{99}	n
ITA	Gaussian	-2172.658	1.359	0.368	0.020	0.057	0.081	0.903	0.931	0.980	247
ITA	Student's t	-2138.430	1.361	0.367	0.012	0.061	0.109	0.895	0.931	0.984	247
ITA	Mixture	-2142.601	1.361	0.367	0.012	0.057	0.097	0.895	0.935	0.984	247
ITA	Stoch. Vol.	-2121.891	1.353	0.370	0.012	0.057	0.101	0.907	0.955	0.992	247
UK	Gaussian	-1723.776	1.356	0.343	0.023	0.068	0.108	0.869	0.919	0.973	222
UK	Student's t	-1725.062	1.363	0.343	0.014	0.072	0.113	0.865	0.914	0.982	222
UK	Mixture	-1726.340	1.358	0.343	0.023	0.068	0.108	0.865	0.919	0.973	222
UK	Stoch. Vol.	-1721.167	1.360	0.343	0.005	0.068	0.117	0.874	0.941	0.991	222

Note: Columns report the cumulative log predictive score (LPS), root mean square error (RMSE), correlation of forecasts and true values (Corr.), and empirical coverage with respect to the predictive 1st, 5th, 10th, 90th, 95th, and 99th quantiles ($q_{01} - q_{99}$), with n denoting the number of non-zero hold-out observations. Results are summaries across out-of-sample periods where $y_{T+1} > 0$ and conditional on $s_{T+1} = 1$.

provides compelling evidence of *persistent* time-varying volatilities in the underlying migration intensity process. This indicates that the process exhibits varying degrees of volatility over time, with some periods characterized by greater stability and others by increased fluctuation.

Under the stochastic volatility model, the empirical tail coverage also closely approximates the expected coverage. It is noteworthy that a very parsimonious model (a count random walk with stochastic volatility) achieves good tail coverage for a very complex and volatile social process. Accurate tail quantile estimates are highly useful in this context as they can be effectively utilized for contingency planning and as risk indicators. The quantile estimates provide useful operational interpretations: the 90th percentile indicates approximately a 10% chance each week of exceeding this threshold, corresponding to an expected exceedance roughly once every 10 weeks (or every 2–3 months). Similarly, the 95th percentile suggests about a 5% weekly probability, translating to one exceedance approximately every 20 weeks (around every 5 months). The 99th percentile implies about a 1% chance each week, suggesting an extreme event approximately once every 100 weeks or nearly once every 2 years.

While these interpretations assume independent weekly observations and are thus approximations, they nonetheless provide valuable indicators that could inform contingency plans. The development of comprehensive operational risk indicators in this domain remains an avenue for future research. From the point of view of statistical (Bayesian) decision theory, an important consideration here is that quantiles are solutions to optimal decision problems under (asymmetric) linear loss functions. If such loss functions could be elicited from the end users of forecasts (migration practitioners or policymakers), even approximately, this could considerably enhance the preparedness capacity of the forecasts (see e.g. [Bijak, 2010](#)).

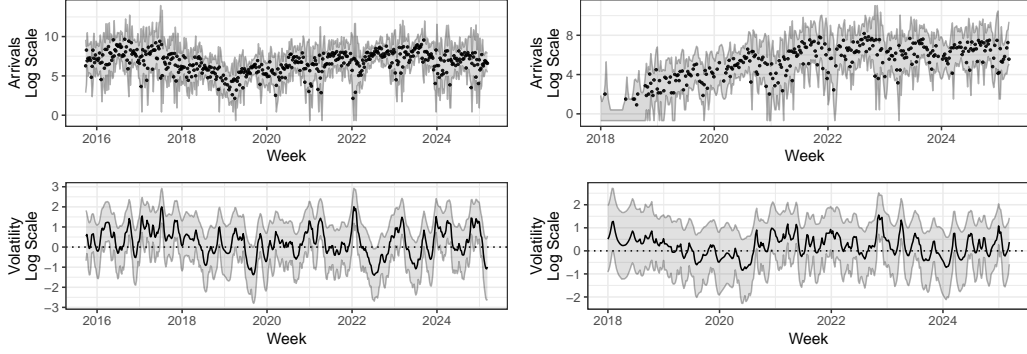


Figure 2: Left top: Non-zero Mediterranean crossing counts and one-step-ahead predictive densities by sample week from 2015W40 to 2025W11. Right top: Non-zero English Channel crossing counts and predictive density by sample week from 2018W01 to 2025W11. Bottom panels: Estimated posterior path of h_t for Mediterranean (left) and UK (right) data. All y -axes are on a log scale. Grey shaded areas are 90% credible intervals.

4.2 Model Fit and Inference on Volatility Patterns

Figure 2 displays one-step-ahead predictive densities for the count data models based on the full posterior of z_{t-1} . For each time point t , this is the predictive density $p(\tilde{y}_t | z_{t-1}, \sigma_t^2, s_t = 1)$, where z_{t-1} is drawn from the full posterior $p(z_{t-1} | \mathbf{y}, \cdot)$, $s_t = 1$ conditions on non-zero outcomes (i.e., the zero-inflation gate being open) and σ_t^2 is the innovation variance implied by f_ϵ at time point t . Additionally, for the stochastic volatility specifications, Figure 2 presents posterior density estimates of the log volatilities $h_t = \log(\sigma_t^2)$, illustrating the time-varying uncertainty captured by these models. These estimates are based on 50,000 posterior samples after an initial burn-in period of 5,000 iterations.

For both the UK and the Mediterranean crossings data, it becomes apparent why the stochastic volatility specification outperforms its competitor models. For the Mediterranean data, the estimated volatility patterns suggest an alternation between periods of high volatility (e.g., beginning of 2022) followed by periods of lower volatility (e.g., mid-2022). Similar patterns, although less pronounced, are found in the UK case study, where the margin by which the stochastic volatility model outperforms the investigated competitors is also somewhat smaller. In both cases, the stochastic volatility process successfully captures the distinction between tranquil and volatile periods, resulting in superior predictive density estimates.

In terms of the zero-inflation component, the estimated posterior mean $\hat{\pi} = 0.96$ for the Mediterranean data indicates that the sampling path is active most of the time. When zeros do occur, the posterior classifies virtually all of them as structural ($s_t = 0$) with (near) probability one. For the UK data, $\hat{\pi} = 0.85$ and approximately all zeros before 2019 are sorted into the sampling zero process ($s_t = 1$), while the zeros after 2019 are sorted into the structural zero process ($s_t = 0$). This reflects that in the beginning of the sample period, the model estimates overall migration intensity to be rather low, and the zeros in the beginning of the sample being produced not due

to a temporary impossibility to cross the English Channel, but due to no migration attempts taking place.

4.3 Explaining Volatility Patterns

To better understand the drivers of time-varying volatility patterns in sea migration data, we perform an additional empirical analysis. We attempt to explain the posterior mean of log volatilities in both case studies through linear regression. Our model incorporates weekly and annual effects along with a quadratic trend to capture seasonal patterns and long-term volatility changes. We also include *ERA5 Reanalysis* variables capturing weather and sea conditions⁴ – wind speed, precipitation, and wave height – measured in the broader crossing regions (see Supplementary Figure S2), as well as their interactions, to assess whether meteorological conditions contribute to increased volatility. Additionally, we include the log of arrival counts to examine whether volatility periods coincide with higher average arrivals or vice versa.

Supplementary Figure S3 presents the results, displaying fitted values for each explanatory variable group and the overall model fit achieved with these covariates. Seasonal patterns, weather and maritime conditions, and annual effects demonstrate some predictive capacity for migration volatility. For the Mediterranean data, we find some evidence that periods of volatility correlate with smaller arrival counts. Overall, the explanatory power of the covariates remains modest, indicating the likely importance of a broader constellation of factors and drivers for the volatility of crossings. The covariates included in the model explain approximately $R^2 \approx 0.50$ of the variance in log volatility posterior means for the Mediterranean and $R^2 \approx 0.37$ for the English Channel. Importantly, both these R^2 values and covariate importance assessments should be interpreted cautiously, as they are overly confident given the regression models do not account for uncertainty in the estimated volatility path.

Our findings thus indicate that at least half of the volatility variation cannot be attributed to long-term trends, annual policy effects, seasonal patterns, or weather and maritime conditions. This substantial unexplained variation likely reflects unmeasured factors including fluctuations in smuggling operations, coast guard activities, and upstream factors affecting the potential migrant population (such as conflict events and political instability). Future work could incorporate a covariate-driven volatility model as an integral model component to strengthen latent volatility estimation, rather than using covariates as inputs for post-hoc exploratory analyses. This approach would present challenges, however, since weather data and observed flow levels become available only retrospectively and would thus also need to be predicted, creating further modeling difficulties.

⁴The data are collected by the European Centre for Medium-Range Weather Forecasts (ECMWF), and are available from <https://cds.climate.copernicus.eu/datasets/reanalysis-era5-single-levels> (as of 7 August 2025).

5 Discussion and Concluding Remarks

5.1 Policy Implications

The empirical evidence in favor of a random walk with persistent time-varying volatility in border crossing activity has several policy implications. First, our finding that irregular migration is well-approximated by a random walk confirms earlier intuitions about the inherent difficulties in predicting these flows (Bijak, 2010). Since random walks imply limited forecastability and rapidly expanding uncertainty with increasing forecasting horizons, turning points may easily be missed, even by elaborate forecasting tools. Consequently, policymakers should avoid relying on medium-run forecasts and rigid annual quotas in reception infrastructure. Instead, the focus should be on building real-time monitoring tools and the provision of flexible surge capacity (e.g., modular reception centers, standby search-and-rescue assets, dynamic solidarity mechanisms) that can scale up or down as the migration process unfolds.

Second, the evidence for persistence in volatility patterns suggests a clustering of calm and volatile periods. Long stretches of low variance and bursts of high variance may alternate. This mirrors the field observation that Mediterranean crossings can be subdued for months and then increase sharply within weeks when, e.g., a civil-war front shifts, a smuggling route re-opens, or a business model of the smuggling gangs changes. From a policy perspective, this suggests treating migration management as risk management, not just as flow management. This would explicitly recognize that the potential *impact* of irregular migration is as important as its *uncertainty and volatility* (see Bijak et al., 2019). During low-volatility windows, policymakers may invest in contingency planning and insurance-type funding (e.g., an EU-wide migration contingency fund) so that cash, assets, and staff are pre-positioned for the next high-volatility spell and are easily scalable to rapidly meet an increasing demand.

Third, a random walk with stochastic volatility generates a heavy-tailed density of outcomes in the sense that extreme events occur more frequently than suggested under standard, homoskedastic models. As such, extreme events such as the 2015 Mediterranean spike or spikes after regime collapses should not be considered as ‘unexpected outliers’ or ‘black swan’ events, but as something that is by construction built into the factors that result in the observed sea border crossing process. As a result, policy should focus on designing systems that are robust to tail risk. Examples include contingency plans that imply sufficient search-and-rescue capacities for ‘worst-case’ scenarios, fast-track legal pathways to siphon off pressure when a surge begins, negotiation of standby humanitarian corridors with coastal states, or trigger-based burden-sharing clauses to reduce pressure on countries of first arrival (e.g., automatic relocation once arrivals cross a pre-defined high percentile). As quantiles remain invariant under monotonic transformations, this can also aid many different practical applications. Moreover, as argued before, quantiles can serve as ready and easily interpretable solutions to statistical decision problems that can be described by using linear loss functions and can therefore approximate many

real-life decision problems in the areas of irregular migration and asylum. The well-calibrated density forecasts that our model provides could provide a useful starting point in that regard.

In summary, by viewing maritime migration through the lens of a random walk with stochastic volatility, the policy focus shifts from forecasting and flow management to risk management and preparedness, as well as from average-case planning to volatility- and tail-risk governance. Note that replacing the unit root assumption with a less stringent, persistent mean-reverting process (e.g., a persistent AR(1) model) only slightly alters these conclusions. Surge capacities and contingency funds remain essential, while predictability of the border crossing process slightly increases. In addition, an AR(1) structure might suggest two added policy levers: (a) actions that can nudge the autoregressive parameter downward – diplomacy in origin states, legal work-migration channels, humanitarian cash transfers – may speed up the natural decay of shocks and spikes; and (b) because large, but not unbounded forecast intervals are now model-consistent, risk-based insurance- and reinsurance-style instruments (e.g., bonds that pay out when arrivals breach a high percentile) can be priced more realistically, especially if coupled with the tenets of statistical decision theory. In short, persistence means shocks linger, yet the faint mean reversion offers room for proactive measures to hasten the return to long-run ‘normality’.

5.2 Model Extensions and Future Research

In conclusion, our dynamic latent variable approach provides a flexible and computationally simple framework for modeling non-stationary, zero-inflated and heteroskedastic count-valued time series. By accounting for time-varying volatility and heavy tails, our model captures key features of the underlying process and delivers well-calibrated predictive performance, particularly for tail events. In our motivating application, these are crucial for policy planning and humanitarian response.

Several avenues are left for future research. Alternative and more complex specifications for f_ε , including asymmetries or a combination of stochastic volatility and heavy tails could be considered. In addition, a dynamic specification for the probability of sampling counts π_t , for example based on dynamic probit models, could be a useful modeling extension that improves predictions. This process, as well as the volatility process, could also be correlated to the count intensity process. Similarly, the conditional mean specification could be explored further by investigating whether a highly persistent, but mean-reverting process outperforms the benchmark RW(1) model we assumed.

Moreover, our analysis has focused on a univariate context, but extensions to multivariate count data frameworks could prove valuable. Applications in migration and border crossing data are numerous; for example, modeling border crossings at different European entry points by different border types and by country of origin could allow for borrowing strength across borders, border types and countries when modeling sparse and noisy high-frequency border crossing processes. In the specific

sea border crossings application context considered here, several modeling choices could be tweaked to further improve log predictive scores or provide even more accurate tail coverage. However, based on our empirical exercises, we are confident that the random walk with persistent, time-varying volatilities will provide a useful, simple, and well-performing benchmarking framework.

On a final note, ethical considerations are paramount when developing models in this domain. Any predictive approach could potentially be considered problematic due to the risk of dual use or misuse, being utilized for advocating for more restrictive border closure policies or repressive measures, or being used by smuggling gangs to inform their operations. That said, as discussed above, border crossing series are barely point-predictable. In the end, these considerations are related to social and political choices, reflecting societal values and negotiated through the democratic process. In addition, these concerns must be weighed against the benefits of increasing preparedness and improved humanitarian resource allocation systems, particularly in the context of sea border crossings. The risk of misuse can further be mitigated through ethical oversight, strict data protection protocols, and inclusive stakeholder engagement to ensure that the models serve public safety and humanitarian goals without infringing on individual rights.

Acknowledgments

The authors gratefully acknowledge Maximilian Böck for insightful discussions that helped shape the early development of this work.

References

- Barra, I., Borowska, A., and Koopman, S. J. (2018). Bayesian dynamic modeling of high-frequency integer price changes. *Journal of Financial Econometrics*, 16(3):384–424.
- Berry, L. R. and West, M. (2020). Bayesian forecasting of many count-valued time series. *Journal of Business & Economic Statistics*, 38(4):872–887.
- Beyer, R. M., Schewe, J., and Lotze-Campen, H. (2022). Gravity models do not explain, and cannot predict, international migration dynamics. *Humanities and Social Sciences Communications*, 9(1):1–10.
- Bijak, J. (2010). *Forecasting International Migration in Europe: A Bayesian View*. Springer.
- Bijak, J., editor (2024). *From Uncertainty to Policy: A Guide to Migration Scenarios*. Edward Elgar.
- Bijak, J., Disney, G., Findlay, A. M., Forster, J. J., Smith, P. W., and Wiśniowski, A. (2019). Assessing time series models for forecasting international migration: Lessons from the united kingdom. *Journal of Forecasting*, 38(5):470–487.

- Bosco, C., Minora, U., Rosińska, A., Teobaldelli, M., and Belmonte, M. (2024). A Machine Learning architecture to forecast Irregular Border Crossings and Asylum requests for policy support in Europe: a case study. *Data & Policy*, 6:e81.
- Camarena, K. R., Claudy, S., Wang, J., and Wright, A. L. (2020). Political and environmental risks influence migration and human smuggling across the Mediterranean Sea. *PloS one*, 15(7):e0236646.
- Carammia, M., Iacus, S. M., and Wilkin, T. (2022). Forecasting asylum-related migration flows with machine learning and data at scale. *Scientific Reports*, 12(1):1457.
- Chan, J. C. and Jeliazkov, I. (2009). Efficient simulation and integrated likelihood estimation in state space models. *International Journal of Mathematical Modelling and Numerical Optimisation*, 1(1-2):101–120.
- Davis, R. A., Holan, S. H., Lund, R., and Ravishanker, N. (2016). *Handbook of discrete-valued time series*. CRC Press.
- Deiana, C., Maheshri, V., and Mastrobuoni, G. (2024). Migrants at sea: unintended consequences of search and rescue operations. *American Economic Journal: Economic Policy*, 16(2):335–365.
- Friebel, G., Manchin, M., Mendola, M., and Prarolo, G. (2024). International migration and illegal costs: Evidence from Africa-to-Europe smuggling routes. *Journal of international economics*, 148:103878.
- Frontex (2024). Migratory Routes. <https://www.frontex.europa.eu/what-we-do/monitoring-and-risk-analysis/migratory-routes/migratory-routes/>.
- Frühwirth-Schnatter, S. and Wagner, H. (2006). Auxiliary mixture sampling for parameter-driven models of time series of counts with applications to state space modelling. *Biometrika*, 93(4):827–841.
- Georgiou, H. V. (2016). Identification of refugee influx patterns in Greece via model-theoretic analysis of daily arrivals. *arXiv preprint arXiv:1605.02784*.
- Hoffmann Pham, K. and Komiyama, J. (2024). Strategic choices of migrants and smugglers in the Central Mediterranean sea. *Plos one*, 19(4):e0300553.
- Jung, R. C., Kukuk, M., and Liesenfeld, R. (2006). Time series of count data: modeling, estimation and diagnostics. *Computational Statistics & Data Analysis*, 51(4):2350–2364.
- Kastner, G. (2016). Dealing with stochastic volatility in time series using the r package stochvol. *Journal of Statistical software*, 69:1–30.
- Kim, S. and Albert, P. S. (2018). Latent variable Poisson models for assessing the regularity of circadian patterns over time. *Journal of the American Statistical Association*, 113(523):992–1002.

- Kim, S., Shephard, N., and Chib, S. (1998). Stochastic volatility: likelihood inference and comparison with ARCH models. *The review of economic studies*, 65(3):361–393.
- Kowal, D. R., Matteson, D. S., and Ruppert, D. (2019). Dynamic shrinkage processes. *Journal of the Royal Statistical Society Series B: Statistical Methodology*, 81(4):781–804.
- McCausland, W. J., Miller, S., and Pelletier, D. (2011). Simulation smoothing for state–space models: A computational efficiency analysis. *Computational Statistics & Data Analysis*, 55(1):199–212.
- Migration Observatory (2025). People crossing the English Channel in small boats. <https://migrationobservatory.ox.ac.uk/resources/briefings/people-crossing-the-english-channel-in-small-boats>.
- Mutiso, F., Pearce, J. L., Benjamin-Neelon, S. E., Mueller, N. T., Li, H., and Neelon, B. (2022). Bayesian negative binomial regression with spatially varying dispersion: Modeling COVID-19 incidence in Georgia. *Spatial Statistics*, 52:100703.
- Neelon, B. (2019). Bayesian zero-inflated negative binomial regression based on Pólya-Gamma mixtures. *Bayesian Analysis*, 14(3):829.
- Roberts, G. O. and Rosenthal, J. S. (2009). Examples of adaptive MCMC. *Journal of computational and graphical statistics*, 18(2):349–367.
- Rodríguez Sánchez, A., Wucherpfennig, J., Rischke, R., and Iacus, S. M. (2023). Search-and-rescue in the Central Mediterranean Route does not induce migration: Predictive modeling to answer causal queries in migration research. *Scientific Reports*, 13(1):11014.
- Schafer, T. L. and Matteson, D. S. (2025). Locally adaptive shrinkage priors for trends and breaks in count time series. *Technometrics*, 67(1):157–167.
- West, M., Harrison, P. J., and Migon, H. S. (1985). Dynamic generalized linear models and Bayesian forecasting. *Journal of the American Statistical Association*, 80(389):73–83.
- Zens, G. and Thalheimer, L. (2025). The short-term dynamics of conflict-driven displacement: Bayesian modeling of disaggregated data from Somalia. *The Annals of Applied Statistics*, 19(1):286–301.

SUPPLEMENTARY MATERIAL

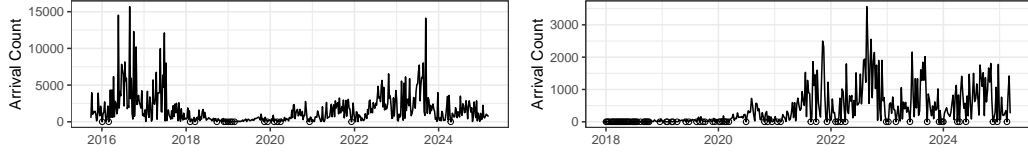


Figure S1: Sea border crossing case study data sets. Left: Mediterranean Sea border crossings to Italy by sample week from 2015W40 to 2025W11. Right: English Channel sea border crossings by sample week from 2018W01 to 2025W11. Panels display counts, with zero counts highlighted as dots on the zero line.

Table S1: Results of the Predictive Exercise: Full Sample.

		LPS	RMSE	Corr.	q_{01}	q_{05}	q_{10}	q_{90}	q_{95}	q_{99}	n
ITA	Gaussian	-2194.909	1.530	0.327	0.000	0.016	0.076	0.900	0.932	0.980	250
ITA	Student's t	-2160.673	1.531	0.326	0.000	0.020	0.076	0.896	0.924	0.984	250
ITA	Mixture	-2164.842	1.532	0.326	0.000	0.012	0.076	0.896	0.932	0.984	250
ITA	Stoch. Vol.	-2144.051	1.524	0.330	0.000	0.016	0.072	0.900	0.956	0.992	250
UK	Gaussian	-1815.361	2.230	0.251	0.000	0.000	0.020	0.876	0.920	0.976	250
UK	Student's t	-1816.002	2.231	0.252	0.000	0.000	0.012	0.872	0.920	0.976	250
UK	Mixture	-1817.786	2.231	0.251	0.000	0.000	0.020	0.872	0.916	0.976	250
UK	Stoch. Vol.	-1812.148	2.231	0.251	0.000	0.000	0.016	0.872	0.932	0.984	250

Note: Columns report the cumulative log predictive score (LPS), root mean square error (RMSE), correlation of forecasts and true values (Corr.), and empirical coverage with respect to the predictive 1st, 5th, 10th, 90th, 95th, and 99th quantiles ($q_{01} - q_{99}$), with n denoting the number of hold-out observations. Results are summaries across out-of-sample periods.



Figure S2: Map showing the boundary boxes for calculating weekly averages of wind speed, precipitation, and wave height in the English Channel (upper box) and the Mediterranean Sea (lower box).

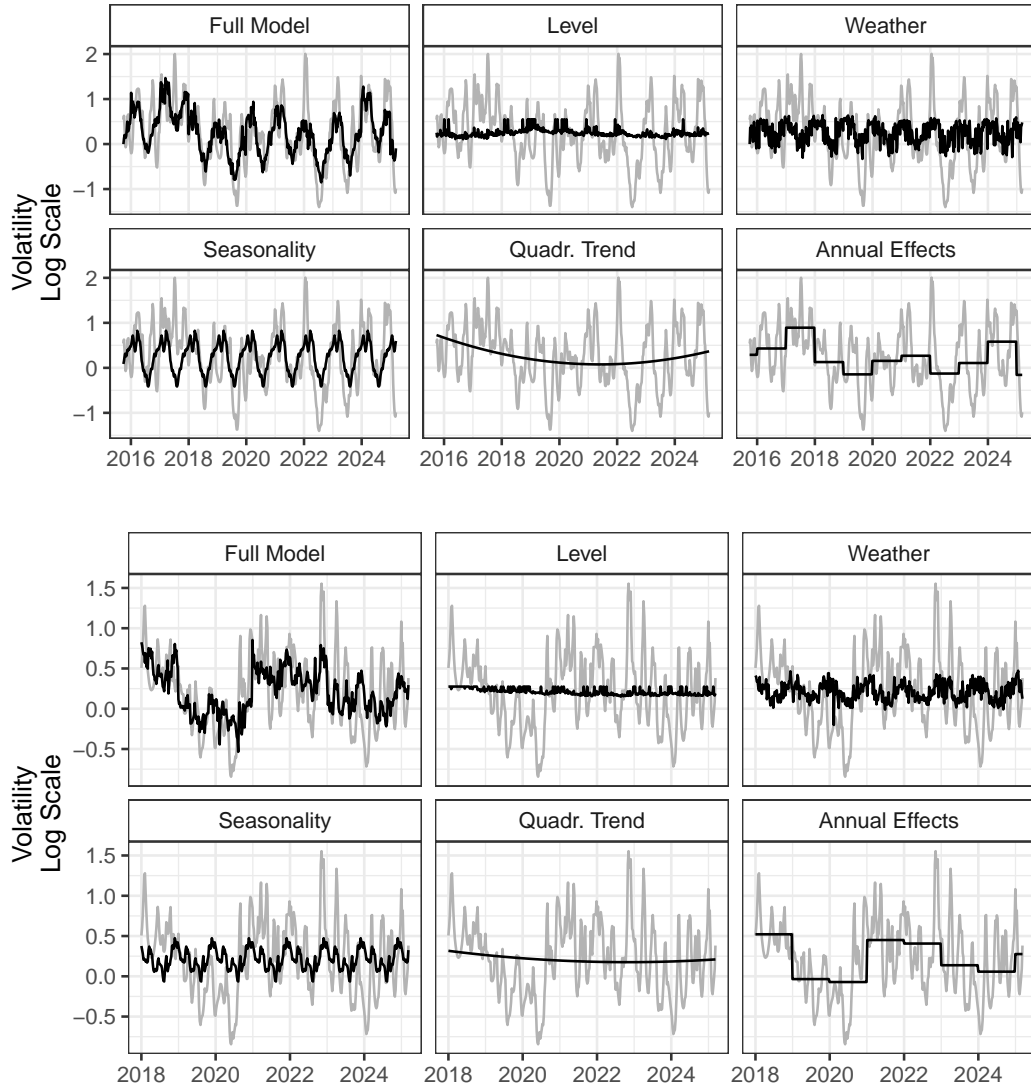


Figure S3: Estimated log-volatility posterior mean (grey) along with fitted values (black) from regressions on the log level of the counts (Level), wave height, wind speed and precipitation as well as their interactions (Weather), weekly seasonal patterns (Seasonality), a quadratic trend, as well as annual effects. 'Full Model' shows the fitted values when all covariates are included in a single regression model. Top: Mediterranean Sea Crossing Data. Bottom: English Channel crossing data.